I3SA: The Increased Step Size Stability Assessment - Applied to the Humanoid Robot REEM-C

Felix Aller[†], Monika Harant[†], Sebastian Sontag[†], Matthew Millard[†] and Katja Mombaur[‡]

***Abstract*— The implementation of stable locomotion is a difficult task. This is complicated by the fact that there is no uniform method for analyzing a robot and its control architecture and for calculating indicators to quantify performance. We propose the Increased Step Size Stability Assessment (I3SA) as a testing protocol and standardized procedure for data collection and evaluation of stability for locomotion on flat terrain. We apply this test to the humanoid robot REEM-C. The biped must cover a set distance of four meters with predefined step sizes. The initial step size is defined as 20 % of the total leg length of the robot. After three successful trials, the step size is continuously increased. This inevitably leads to a fall as soon as the robot can no longer accomplish the task under the selected conditions. The recorded data are evaluated using metrics known from the literature, such as the capture point, foot placement estimator and the angular momentum acting at the center of mass. We illustrate the experimental setup, data collection and aggregation, the calculation of performance indicators for several step sizes and the trial which resulted in a fall of the robot. The trend towards decreasing stability with increased step size and the available key assumptions are reported.**

I. INTRODUCTION

Performance testing and benchmarking will be as critical to the field of robotics in the future as it currently is for the automotive industry. A human-sized robot that loses its balance and falls on a person could cause just as much injury as a car accident. Benchmarking describes the process of a standardized assessment of systems on the basis of performance indicators. In order for a robot to operate in a human environment, reliable locomotion is a crucial goal for the design of humanoid robots [1]. Unfortunately, there is no publicly available test that can be used to challenge a robot's balance and measure its response.

Current efforts dedicated to the assessment of a robot's performance are mostly determined using competition [2]. This type of evaluation is an important part of determining performance on goal-oriented tasks and is a driving factor in robotics research [3]. Challenges such as the DARPA Robotics Challenge [4], the Robot Soccer Cup [5], the SciRoc challenge [6] or the Cybathlon event [7] are important holistic evaluations of robotic performance. Unfortunately, competitions usually do not include a detailed assessment and a quantitative evaluation of the many abilities a robot needs to function.

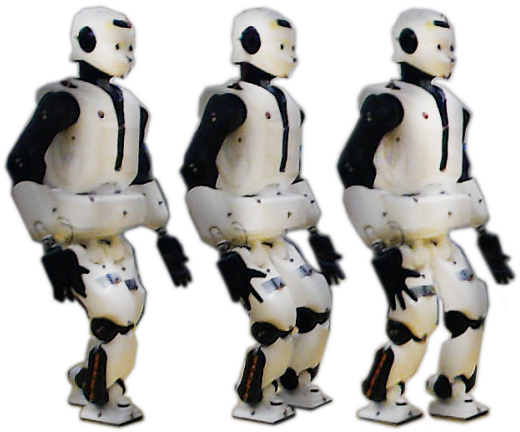

Fig. 1. REEM-C Robot performing the I3SA protocol.

Several research labs have begun to formulate tests to evaluate walking stability on inclinations, balance recovery, and efficiency. Dutta et al. analyze robot-body stability on inclined surfaces [8]. A modular teststand for human posture control and balance assessment is presented by Lippi et al. [9]. Peng et al. evaluate the ability to enter a steppable state from an unbalanced state of the humanoid robot DARwIn-OP[10]. Walking efficiency is being investigated by Tacué et al. using a statistical comparison of energy expenditure for different pattern generators for bipedal robots [11]. While this growing list of tests is important, the tests specifically do not evaluate the limits of the robot's stability by increasing the difficulty of the test until a fall occurs. To date no published evaluations of humanoid robots have made their hardware designs and evaluation software open-source.

We propose the Increased Step Size Stability Assessment (I3SA) consisting of a physical test that can be carried out in any lab and provide open-source implementations as a part of the EUROBENCH[1] project. To illustrate the utility of the test, we apply it to the humanoid robot REEM-C (Fig. 1) and increase the difficulty until REEM-C can no longer perform the requested motion and thus falls.

In the following Section II, the routines for data collection and aggregation, the experimental setup, and the computation of implemented stability metrics are described. The results of the metrics for increasing gait difficulty are presented

*This work was supported by the project EUROBENCH (European Robotic Framework for Bipedal Locomotion Benchmarking, www.eurobench2020.eu) funded by H2020 Topic ICT 27-2017 under grant agreement number 779963.

[†]Felix Aller, Monika Harant, Sebastian Sontag and Matthew Millard are with the Optimization, Robotics and Biomechanics Chair, Institute of Computer Engineering, Heidelberg University, Heidelberg, Germany felix.aller@ziti.uni-heidelberg.de

[‡]Katja Mombaur, Canada Excellence Research Chair in Human-Centred Robotics and Machine Intelligence, Faculty of Engineering, University of Waterloo, Waterloo, Canada katja.mombaur@uwaterloo.ca

[1]http://eurobench2020.eu/

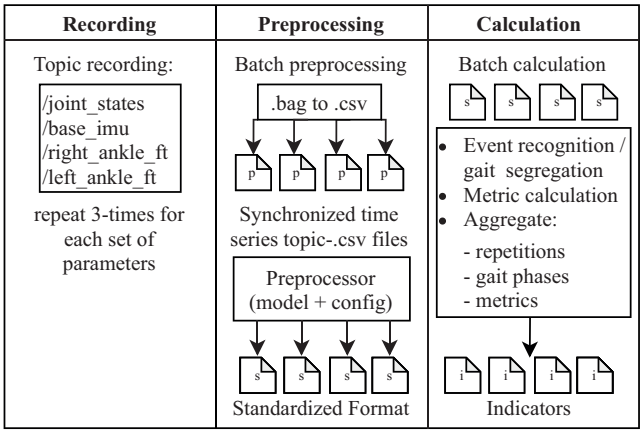

Fig. 2. **Recording:** Robot-specific data are queried directly from the robot and, in the case of REEM-C (ROS based), stored in the rosbag file format. **Preprocessing:** All rosbag files are batch processed into time series files containing the sensory information. A preprocessing routine injects the global translation and orientation of the robotic base link to the data, fits cubic smoothing splines in order to calculate derivatives or uses inverse dynamics to calculate joint torques. **Calculation:** Based on the standardized format the metrics are calculated by segregation of gait phases based on events and an aggregation of all gait phases and trials to obtain performance indicators.

in Section III. Section IV elaborates on key findings from the trials. In Section V, we conclude with the performance evaluation of the robot and future work.

II. I3SA BENCHMARKING PROTOCOL AND PERFORMANCE INDICATORS

The presented benchmarking protocol assesses the biped's stability during flat-ground walking as a result of the large interest in these topics in the robotics literature [12]. Within this protocol, the robot has to cover a fixed distance of 4 meters several times (Fig. 3). The step size, which is defined by the maximum length between both ankles at the double support phase, and the number of steps are fixed, beginning and ending at rest. The initial starting condition requires the robot to use 20 % of the robot's leg length as step size to cover the 4 meters. The step size is gradually increased after every three successful trials, decreasing the required step amount and eventually leading to a loss of balance. If the robot cannot span the distance with the specified step size within the three trials, the protocol is concluded. At the end of each trial, the robot is returned to the same starting point by means of a personnel lift. This experimental setup also serves as a pilot project to integrate such assessments into the EUROBENCH framework.

At low step numbers this test will become difficult even for very athletic humans: the hardest version of this test requires a standing long jump of 4 m, which exceeds even the current world record of 3.73 m held by Byron Jones [13]. In the case of the robot used, this results in five experiments (Tab. I) with the individual step sizes, corresponding step numbers , step durations, complete gait cycles obtained, total distances traveled, and the total experiment duration. The fall of the robot occurred in the third trial at 40% of the total leg length, which corresponds to a step size of 34.34 cm (Fig. 6).

TABLE I
I3SA - OVERVIEW OF TRIAL CONDITIONS

%	Step			Total		
Leg	**Size**	**Count**	**Time**	**Cycles**	**Distance**	**Time**
20	17.17 cm	24	1.00 s	12	4.12 m	25.2 s
25	21.46 cm	19	1.00 s	9	4.07 m	20.5 s
30	25.75 cm	16	1.00 s	7	4.12 m	16.1 s
35	30.04 cm	14	1.04 s	6	4.24 m	14.5 s
40	34.34 cm	12	1.15 s	5	4.12 m	13.8 s

The commercially available adult-sized humanoid robot REEM-C (Fig. 1), manufactured by PAL Robotics, serves as a platform for the experiment. The source of data for the experimental evaluation originates from the internal sensors of the robot. Therefore, no external measurement systems are needed. Position and velocity information are obtained from the robot's motor encoders and the ground reaction forces and moments from a 6-axis force-moment sensor on the sole of each foot of the robot. Acceleration data are obtained by deriving a cubic smoothing spline fit to the velocity data. Global position and orientation are reconstructed from an internal IMU located at the center of the robot's pelvis segment providing acceleration, angular rates and the magnetic field. We verified the accuracy of the provided data:

- The motor encoders were validated with a motion capture system by analyzing the lower body segments: the two systems are within $0.5^\circ \pm 0.39^\circ$ of each other.
- The force-torque sensors were validated using a force plate: We calculated and compared the center of pressure during a crouching motion (1) and two static poses where the robot stands on the left (2) and right (3) foot. The two systems are within 1.13 ± 0.071 (1), 0.70 ± 0.078 (2) and 0.86 ± 0.027 (3) cm of each other.
- The IMU readings were captured with the robot at rest: No significant drift of the sensors could be detected during a one-minute recording.

The reconstructed motion is split into separate phases identified by the events of toe off and touch down of the left or right foot ($TD_{L/R}$, $TO_{L/R}$, respectively). We define $TD_{L/R}$ to have occurred when the normal forces measured by the robot's force torque sensor to register equal or more than 10 N and $TO_{L/R}$ less than 10 N. We analyze the complete gait phase which is defined as a combination of the phases of two legs between $TO_R(n)$ and $TO_R(n+1)$ containing the:

- swing phase of the right leg after $TO_R(n)$,
- double support phase after $TD_R(n)$,
- the swing phase of the left leg after $TO_L(n)$,
- and the double support phase after $TD_L(n)$, recorded until the last time instance before $TO_R(n+1)$,

with n being the $n-$th gait phase. The reported results are described according to the aggregated data of all complete gait phases for all trials corresponding to the same step size. For the trial in which the fall occurred, we report the complete gait cycle up to the estimated time of tipping over. The first and last half-step of the trajectory that lead into and end a full gait cycle are discarded. In hopes of having

this test widely adopted, we have used open-source software tools, such as the Robotic Operating System (ROS) for data collection and the Rigid Body Dynamics Library (RBDL) for assessment [14]. All file formats are generalized according to the standardized EUROBENCH input file format[2] and all metrics are calculated a posteriori regardless of the robots' underlying control architecture (Fig. 2).

A. Applied Performance Indicators

Quantifying dynamic stability is challenging. We refer to commonly used indicators in robotics and evaluate the dynamic stability of the robot during the experiment by the following:

Center of Pressure (CoP) / Zero Moment Point (ZMP): As described by Sardain and Bessonnet [15] the two forces acting on the biped can be divided into the categories of forces exerted by contact and forces transmitted without contact, which are described by the CoP and the ZMP, respectively. Both are typically used to achieve dynamic stability by controlling the dynamic equilibrium of the biped. As described by Sardain and Bessonnet [15] and Vukobratovic et al. [16], the ZMP location ($\underline{r}_Z$) is coincident with the CoP location ($\underline{r}_P$) as long as the robot is dynamically stable, referring to this point as CoP-ZMP. The CoP-ZMP is the point on the ground at which the tipping moment acting on the robot is zero due to gravity and inertial forces. When the CoP-ZMP reaches the edge of the base of support (BoS), the contact cannot be maintained and the biped begins to tip over the edge of the BoS, causing the system to become unstable. Since $\underline{r}_Z$ is always an approximation based on the inertia information, the quality of $\underline{r}_Z$ is highly model dependent. Instead of calculating $\underline{r}_Z$, we use the force torque sensors on both the robot soles to calculate $\underline{r}_P$, since the sensory information seems more reliable and also serves as basis for the walking controller used, being well aware that both locations should ideally coincide. To verify the assumption that the foot of the stance leg is flat on the ground, i.e. the sole is parallel to the ground-plane, we verify whether the angular velocity about the horizontal axes of the stance foot ω_{foot} remains small.

Capture Point (CP): The CP defines the point on the ground where the robot must step in order to come to a complete stop [17] assuming its center of mass (CoM) trajectory follows a straight line. The CP location ($\underline{r}_C$) allows the humanoid to control the angular momentum acting on the CoM and calculates where the foot should be placed with respect to the CoM to reach a statically stable standing position. By constraining the CoM to travel in a straight line the CP assumes that the orbital energy is conserved [18].

Foot Placement Indicator (FPE): The FPE improves upon the CP by considering both linear and angular momentum. The location of the FPE ($\underline{r}_F$) can be used to describe the dynamic stability margin relative to the BoS, considering the specific foot position and the dynamics of motion [19]. Both, $\underline{r}_C$, $\underline{r}_F$ also allow to assess situations where $\underline{r}_P$ already reached the edge of the BoS and indicates a tipping-over moment. The FPE assumes that the state the biped's body can be projected on the vertical plane without information loss. This is the case if the angular momentum of the robot acting in the vertical direction when evaluated by the ground projected CoM, stays low. The projection error depicts the percentage of the vertical component of the angular momentum and thus the rate of failure of this projection. We evaluate the dynamic margin of stability by calculating the distance between each of these points and the nearest BoS edge (d_{BP}, d_{BC}, d_{BF}, respectively) and use a positive sign to indicate that the point is within the BoS. The physical interpretation of these distances is the same for both the d_{BF} and d_{BC}: as long as the distance is positive the robot is dynamically stable; if the distance is negative the robot needs to take a step to catch its balance and prevent a fall. In contrast, d_{BP} must be greater than zero for the robot to be dynamically stable: a distance of zero indicates that $\underline{r}_P$ is on a foot edge and the robot is going to fall. A robot that displays a superior ability to balance will be able to to walk with $d_{BP} > 0$ and tolerate larger negative excursions of d_{BC} and d_{BF} and higher velocities without falling than a robot with a poorer sense of stability.

Angular Momentum (AM): People seem to minimize their AM during walking [20], making this quantity a valuable source of information. Therefore, we report the normalized angular momentum about the CoM by $m \cdot l^2$ about the longitudinal axis AM_x, lateral axis AM_y, and vertical axis AM_z, with m being the mass of the robot at 77.5 kg and l as total leg length from sole to the base link in null pose at 85.85 cm. Moreover, this information becomes even more valuable when the maximum angular momentum is calculated, which allows to obtain information on the reserved angular momentum left to perform push recovery motions [21].

In addition, we evaluate the key assumption mentioned for each indicator as it is currently not clear which method is best suited for analyzing robotic movements.

III. EXPERIMENTAL RESULTS

Across all successful trials the robot has the smallest margin of stability between $TO_{L/R}$ and $TD_{L/R}$, and the highest margin of stability at mid stance of each double support phase (Fig. 4). A decrease in stability can be observed for the 34.34 cm step size as d_{BP} does not recover as quickly after TD_R (with $\underline{r}_P$ being closer to the BoS). Therefore, a trend can be observed at d_{BP} for the 17.17 cm step size recovering the earliest with 25.75 cm step size following closely. The 34.34 cm step size can not validate this trend and therefore d_{BP} is more than 2 cm smaller at mid double support phase. This results in a worse performance of the 34.34 cm step size in the pre-mid phase of the second swing after TO_L. This culminates in the fall trial with the lowest values for d_{BP} of all trials during the double support phase. Therefore, no recovery was achieved and the robot tips over during the first double support phase which is also underlined by the high values of the angular momentum around all axes (Fig.

[2]https://eurobench.github.io/sofware_documentation/latest/

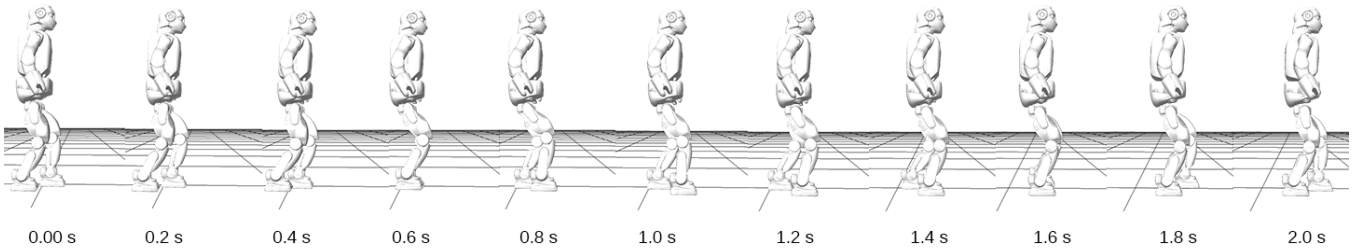

Fig. 3. Complete gait cycle within the 25.75 cm step size trial. The swing phase of the right leg followed by double support phase at $0.0-1.0$ corresponds to $0-0.51$ (Fig. 4) and the swing phase of the left leg followed by double support phase at $1.0-2.0$ corresponds to $0.52-1.0$ (Fig. 4).

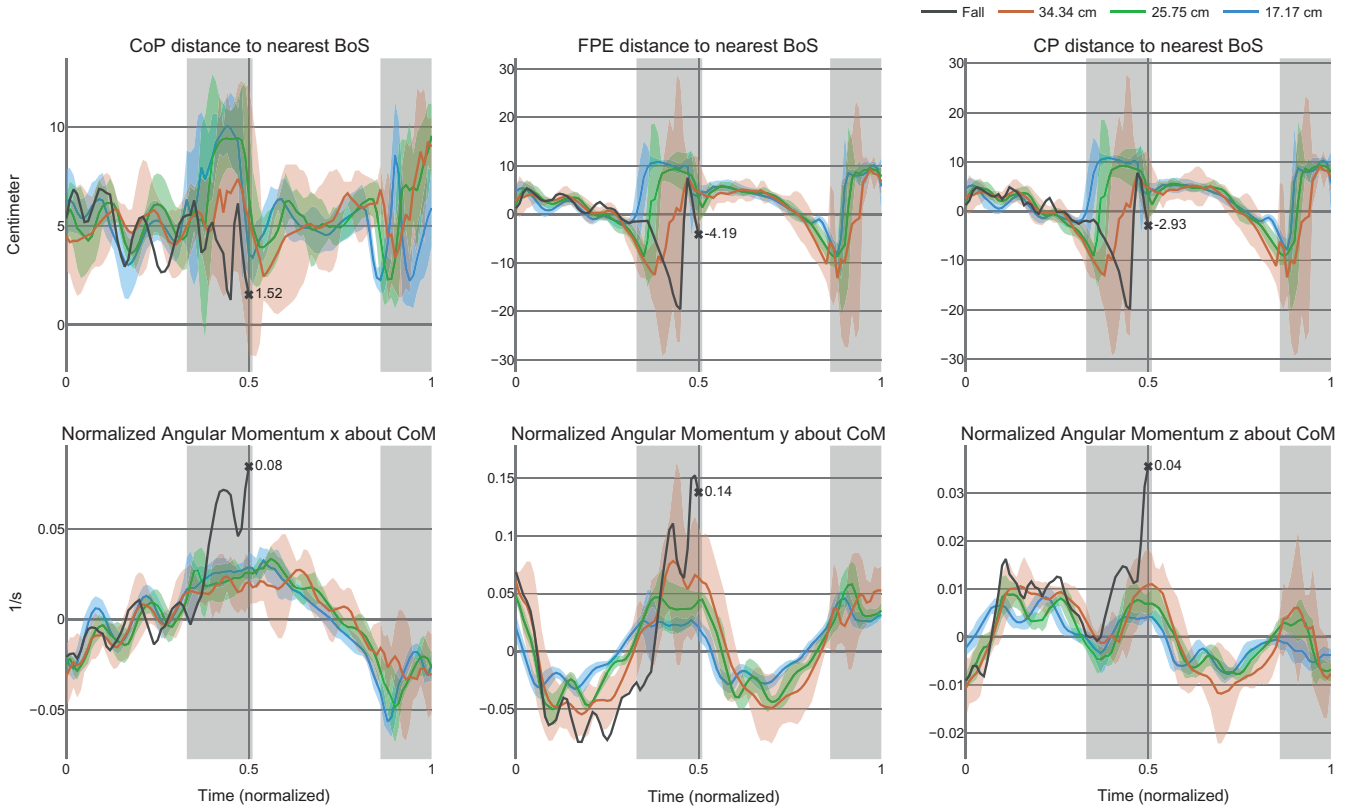

Fig. 4. All plots show three representative walking trials from the five experiments conducted and the falling trial. All trials with respect to a step size and all associated phases $TO_R(n)$ to $TO_R(n+1)$ are normalized. The two double support phases between the swing phases of the right and left leg are indicated in gray. The data in the plots are surrounded by a 95 % confidence area. The estimated moment of no return which results in a fall of the robot is indicated at $\times$ with the respective value at the time of fall. From the top left to the bottom right we visualize the calculated distances from points of interest to the BoS: d_{BP}, d_{BF} and d_{BC} in cm, followed by the angular momentum normalized by $m \cdot l^2$ in $1/s$ about all axes, AM_x, AM_y, AM_z, and the angular velocity of the stance foot ω_{foot} about all axes in $^\circ/s$.

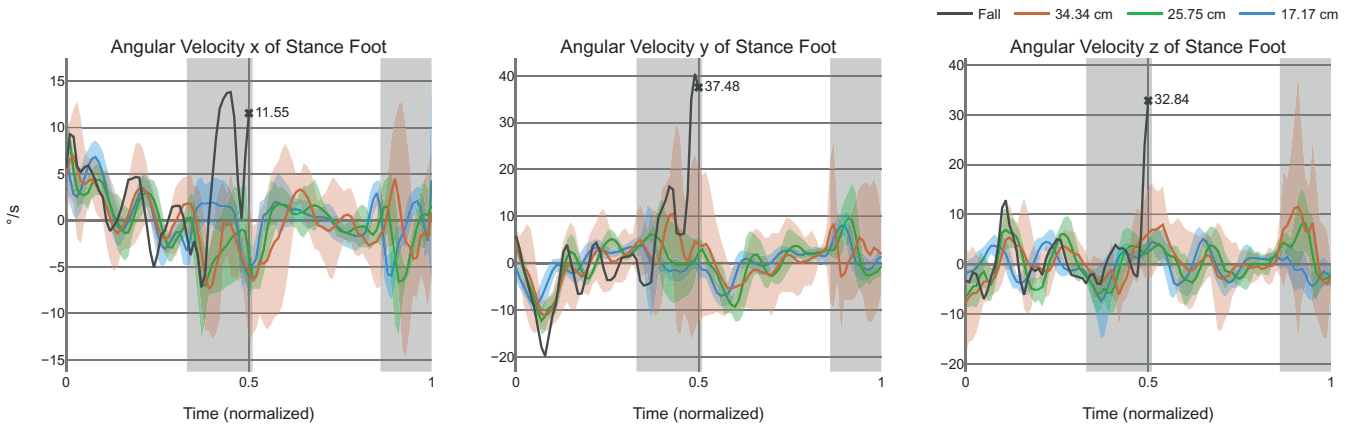

Fig. 5. Angular velocity of ω_{foot} about all axes in $^\circ/s$ to verify the assumption that the foot of the stance leg is flat on the ground.

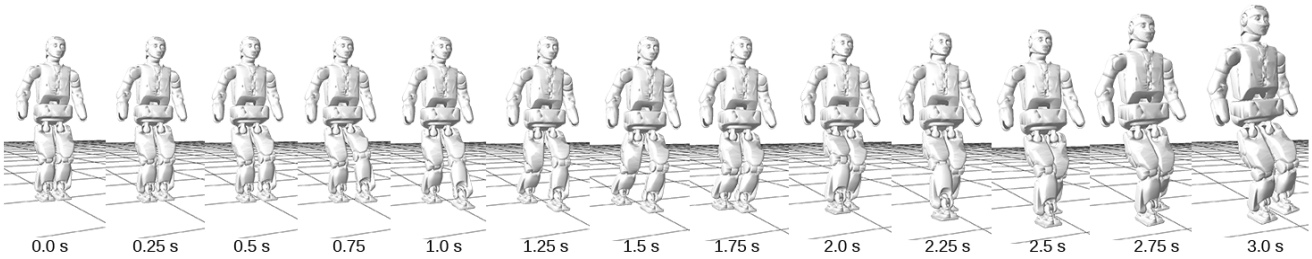

Fig. 6. Complete experiment at step size of 34.34 cm which resulted in tipping over of the robot by a rotation about the lateral axis in gait direction. The period from 1.5 s to 2.5 s (tipping over point) corresponds to the fall trial in the data plots (Fig. [4, 5, 7]).

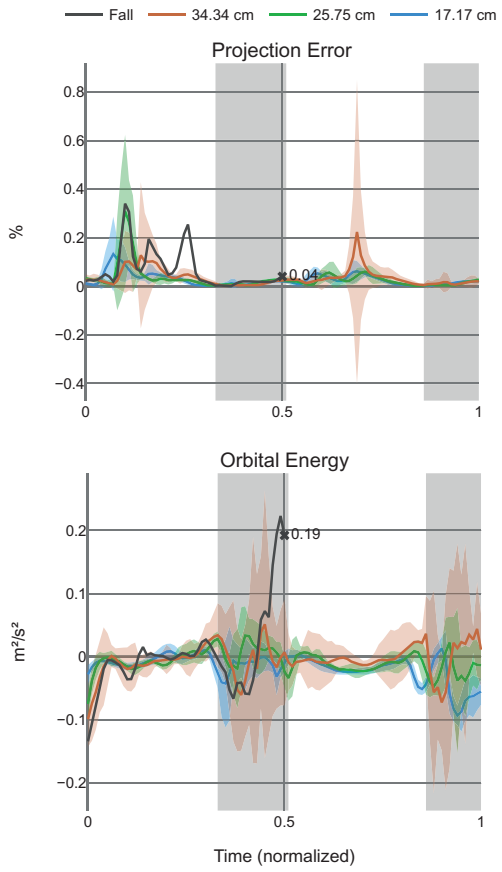

Fig. 7. Two plots visualize the projection error and the orbital energy to clarify assumptions for three representative step sizes and the falling trial.

4). For the successful trials at a step size of 34.34 cm, the robot could recover after the mid-phase of the second swing phase (after TO_L) and even improve upon the smaller step sizes in the following double support phase (after TD_L) with 17.17 cm being at the lowest stability margin. By comparing $min(d_{BP})$ (Tab. II) however, we could not identify a clear characteristic between all the different trials.

The behavior is different for all step sizes by analyzing d_{BF} and d_{BC}, which also closely match (Fig. 4). d_{BC} shows a more choppy behavior for the fall trial during the first single support phase (after TO_R). During both swing phases the indicators become negative after mid-phase for all step sizes indicating that the robot needs to take a step not to lose balance. The comparison of the step sizes at $min(d_{BC})$

TABLE II

RESULTS FOR THE RIGHT SWING AND DOUBLE SUPPORT PHASE

Indicators	**Step Size (cm)**				
	17.17	**21.46**	**25.75**	**30.04**	**34.34**
$min(d_{BP})$ $[cm]$	1.69	2.66	2.13	2.22	1.86
$min(d_{BC})$ $[cm]$	-5.93	-6.99	-10.841	-14.95	-32.58
$min(d_{BF})$ $[cm]$	-6.06	-7.09	-10.70	-14.72	-33.75
$max(\frac{d}{dt}(d_{BF}))$ $[cm/s]$	4.01	3.90	4.78	5.34	6.80
$max(\lvert AM_x \rvert)$ $[1/s]$	0.035	0.039	0.036	0.044	0.046
$max(\lvert AM_y \rvert)$ $[1/s]$	0.046	0.059	0.067	0.090	0.162
$max(\lvert AM_z \rvert)$ $[1/s]$	0.010	0.009	0.012	0.019	0.016

and $min(d_{BF})$ also reflects this trend. More interestingly we observe different recovery speeds during first double support phase after TD_R and an increasing delay for greater step sizes which eventually is leading to a fall. This observation is supported by $max(\frac{d}{dt}(d_{BF}))$ which is steadily increasing for greater step sizes. Again, the two smaller step size trials agree more closely whereas the larger step size diverges further from a fast recovery rate. The AM around the CoM indicates symmetrical movements for the swing phases of both legs. A trend towards greater AM_y can be observed at $max(\lvert AM_y \rvert)$ for increasing step sizes.

Three different quantities ω_{foot}, projection error, and orbital energy were selected to assess how well the assumptions were met that are made during indicator calculation: The mean ω_{foot} over the gait cycles remains under 15 $^\circ/s$ throughout the whole gait cycle for all successful trials indicating only a small twisting and turning of the stance foot. For the fall trials, the angular velocity of the foot reaches 40 $^\circ/s$ showing a clear tipping over of the robot (Fig. **??**). The projection error of the FPE shows two spikes for 34.34 cm step size but only one spike at the beginning of the swing phase after TO_R for smaller step sizes (Fig.7). Otherwise, it remains low (under 0.1 %) for the gait cycle justifying the approximation made during the calculation of $\underline{r}_F$. The orbital energy is not constant but positive during breaking and making contact and stays the most negative until mid-stance for a step size of 17.17 cm (Fig. 7).

IV. DISCUSSION

Our work demonstrates that the I3SA protocol is a suitable procedure to generate data and to evaluate the performance of robot stability by means of a uniform and basic setup. The position and force reconstruction using motor encoder data,

IMU, and force torque sensors works accurately and reliably. Thus, it is possible to record a robotic system without the addition of external measuring devices, after the internal sensors have been verified against such devices once. The generalized file format further supports the analysis of data from different sources, be it robot internal sensors or external measurement systems.

The I3SA results illustrate trends in performance by analyzing the outputs of the methods presented, but also limitations of the latter. Overall, it can be observed that although the trend of the metrics, clearly indicates a deterioration of the stability, the results cannot predict a fall of the robot with certainty.

Nevertheless, interesting properties of the robot's gait could be identified: A slight rotation of the stance leg around all axes exists across all step sizes, which also triggered the fall. A weight shift between the legs started early on, even before the stance foot was aligned parallel to the ground. This behavior already occurred in functioning trials, but this fact is compensated by the foot shape of REEM-C, which allows a roll-off similar to human gait due to its rounded shape at the heel and front of the foot. The AM behaves similar to humans as well. Similar signatures to the curves resembling those of human gait [20] can be recognized. The walking controller used in this experiment utilizes a stabilizer that implements minimal motion compensation accommodating slight mechanical inaccuracies or small irregularities on the ground. However, it is far from being able to compensate for bigger disturbances or to perform push recovery. For this purpose, the analysis of the angular momentum becomes even more important in the further course of our research: When controllers which implement advanced recovery strategies, it is important to know the reserves of angular momentum for possible compensation movements.

V. CONCLUSIONS

With the evaluated stepping controller, the results of the I3SA protocol indicate that REEM-C is able to accomplish steps of various sizes, some of which amount to 40% of his total leg length. The performance degradation to the last possible step size is low and the angular momentum symmetrical, which speaks for the reliability of the controller and robot. Future work will include the analysis of more advanced walking controllers with the same methods, but also different robots with different types of actuators and additional performance indicators that also take into account kinetic properties to allow a broad comparison of bipedal locomotion.

REFERENCES

[1] D. Torricelli, J. Gonzalez, M. Weckx, R. Jiménez-Fabián, B. Vanderborght, M. Sartori, S. Dosen, D. Farina, D. Lefeber, and J. L. Pons, "Human-like compliant locomotion: state of the art of robotic implementations," *Bioinspiration & biomimetics*, vol. 11, no. 5, p. 051002, 2016.

[2] A. P. del Pobil, R. Madhavan, and E. Messina, "Benchmarks in robotics research," in *Workshop IROS*. Citeseer, 2006.

[3] S. Behnke, "Robot competitions - ideal benchmarks for robotics research," 2006.

[4] "Darpa Robotics Challenge," https://www.darpa.mil/program/darpa-robotics-challenge, accessed: 2021-03-01.

[5] "Robot Soccer Cup," https://www.robocup.org/, accessed: 2021-03-01.

[6] "SciRoc Challenge," https://sciroc.org/, accessed: 2021-03-01.

[7] "Cybathlon," https://cybathlon.ethz.ch/, accessed: 2021-03-01.

[8] S. Dutta, T. K. Maiti, M. Miura-Mattausch, Y. Ochi, N. Yorino, and H. J. Mattausch, "Analysis of Sensor-Based Real-Time Balancing of Humanoid Robots on Inclined Surfaces," *IEEE Access*, vol. 8, pp. 212 327–212 338, 2020.

[9] V. Lippi, T. Mergner, T. Seel, and C. Maurer, "COMTEST Project: A Complete Modular Test Stand for Human and Humanoid Posture Control and Balance," in *2019 IEEE-RAS 19th International Conference on Humanoid Robots (Humanoids)*. IEEE, 2019, pp. 630–635.

[10] W. Z. Peng, C. Mummolo, and J. H. Kim, "Stability criteria of balanced and steppable unbalanced states for full-body systems with implications in robotic and human gait," in *2020 IEEE International Conference on Robotics and Automation (ICRA)*. IEEE, 2020, pp. 9789–9795.

[11] J. Tacué, C. Rengifo, and D. Bravo, "An experimental energy consumption comparison between trajectories generated by using the cart-table model and an optimization approach for the bioloid robot," *International Journal of Advanced Robotic Systems*, vol. 17, no. 2, p. 1729881420917808, 2020.

[12] F. Aller, D. Pinto-Fernandez, D. Torricelli, J. L. Pons, and K. Mombaur, "From the State of the Art of Assessment Metrics Toward Novel Concepts for Humanoid Robot Locomotion Benchmarking," *IEEE Robotics and Automation Letters*, vol. 5, no. 2, pp. 914–920, 2019.

[13] "Current world record of the standing long jump," https://en.wikipedia.org/wiki/Standing_long_jump, accessed: 2021-03-01.

[14] M. L. Felis, "RBDL: an efficient rigid-body dynamics library using recursive algorithms," *Autonomous Robots*, vol. 41, no. 2, pp. 495–511, 2017.

[15] P. Sardain and G. Bessonnet, "Forces acting on a biped robot. center of pressure-zero moment point," *IEEE Transactions on Systems, Man, and Cybernetics-Part A: Systems and Humans*, vol. 34, no. 5, pp. 630–637, 2004.

[16] M. Vukobratović and B. Borovac, "Zero-moment point—thirty five years of its life," *International journal of humanoid robotics*, vol. 1, no. 01, pp. 157–173, 2004.

[17] J. Pratt, J. Carff, S. Drakunov, and A. Goswami, "Capture point: A step toward humanoid push recovery," in *2006 6th IEEE-RAS international conference on humanoid robots*. IEEE, 2006, pp. 200–207.

[18] S. Kajita and K. Tani, "Study of dynamic biped locomotion on rugged terrain-derivation and application of the linear inverted pendulum mode," in *Proceedings. 1991 IEEE International Conference on Robotics and Automation*. IEEE Computer Society, 1991, pp. 1405–1406.

[19] M. Millard, J. McPhee, and E. Kubica, "Foot placement and balance in 3D," *Journal of computational and nonlinear dynamics*, vol. 7, no. 2, 2012.

[20] H. Herr and M. Popovic, "Angular momentum in human walking," *Journal of experimental biology*, vol. 211, no. 4, pp. 467–481, 2008.

[21] J. E. Pratt and R. Tedrake, "Velocity-based stability margins for fast bipedal walking," in *Fast Motions in Biomechanics and Robotics*. Springer, 2006, pp. 299–324.